Centre of pressure modulations in double support effectively counteract anteroposterior perturbations during gait

van Mierlo, M.; Vlutters, M.; van Asseldonk, E. H.F.; van der Kooij, H.

DOI
10.1016/j.jbiomech.2021.110637

Publication date
2021

Document Version
Final published version

Published in
Journal of Biomechanics

Citation (APA)
van Mierlo, M., Vlutters, M., van Asseldonk, E. H. F., & van der Kooij, H. (2021). Centre of pressure modulations in double support effectively counteract anteroposterior perturbations during gait. *Journal of Biomechanics*, *126*, Article 110637. https://doi.org/10.1016/j.jbiomech.2021.110637

Journal of Biomechanics 126 (2021) 110637

Contents lists available at ScienceDirect

Journal of Biomechanics

journal homepage: www.elsevier.com/locate/jbiomech

Centre of pressure modulations in double support effectively counteract anteroposterior perturbations during gait

M. van Mierlo [a,*], M. Vlutters [a], E.H.F. van Asseldonk [a], H. van der Kooij [a,b]

[a] Department of Biomechanical Engineering, University of Twente, Enschede, The Netherlands
[b] Department of Biomechanical Engineering, Delft University of Technology, Delft, The Netherlands

ARTICLE INFO

Keywords:
Human balance
Double support
Centre of pressure
Linear inverted pendulum model

ABSTRACT

Centre of mass (CoM) motion during human balance recovery is largely influenced by the ground reaction force (GRF) and the centre of pressure (CoP). During gait, foot placement creates a region of possible CoP locations in the following double support (DS). This study aims to increase insight into how humans modulate the CoP during DS, and which CoP modulations are theoretically possible to maintain balance in the sagittal plane. Three variables sufficient to describe the shape, length and duration of the DS CoP trajectory of the total GRF, were assessed in perturbed human walking. To counteract the forward perturbations, braking was required and all CoP variables showed modulations correlated to the observed change in CoM velocity over the DS phase. These correlations were absent after backward perturbations, when only little propulsion was needed to counteract the perturbation. Using a linearized inverted pendulum model we could explore how the observed parameter modulations are effective in controlling the CoM. The distance the CoP travels forward and the instant the leading leg was loaded largely affected the CoM velocity, while the duration mainly affected the CoM position. The simulations also showed that various combinations of CoP parameters can reach a desired CoM position and velocity at the end of DS, and that even a full recovery in the sagittal plane within DS would theoretically have been possible. However, the human subjects did not exploit the therefore required CoP modulations. Overall, modulating the CoP trajectory in DS does effectively contributes to balance recovery.

1. Introduction

Healthy humans have excellent capabilities to maintain balance and avoid falling during walking. They use various balance strategies to recover from perturbations and control their centre of mass (CoM) motion (Pollock et al., 2000). The direction and magnitude of the ground reaction force (GRF) and its point of application, the centre of pressure (CoP), influence the CoM position and velocity over time (Hof, 2007; Jian et al., 1993). An extensively studied balance strategy is foot placement. Together with the length and width of each foot it sets the base of support (BoS), determining the possible future CoP locations for the upcoming gait phases (Hof et al., 2005).

The importance of foot placement to counteract perturbations is less evident in the sagittal plane than in the frontal plane (Arvin et al., 2018; Bruijn and Dieën, 2018; Hof, 2007; Hof and Duysens, 2013; Hof et al., 2010; Tokur et al., 2020; Vlutters et al., 2016). No significant foot placement modulations with respect to the CoM were seen after anteroposterior (AP) perturbations during walking (Vlutters et al., 2016). Instead, various studies emphasize the use of the ankle strategy in the sagittal plane to modulate the CoP within the BoS, following foot placement (Gruben and Boehm, 2014; Hof et al., 2005; Matjačić et al., 2017; Millard et al., 2009; Vlutters et al., 2016). These studies clearly demonstrate CoP modulations after balance perturbations. However, how these modulations relate to changes in the CoM position and velocity was not investigated.

Although the CoP position changes during the whole stance phase, the largest displacement is observed during double support (DS), when the CoP transfers from the trailing to the leading foot. During DS the ankle strategy and weight shift influence the CoP position (Hof, 2007). When DS takes longer, there is more time for CoP adjustments influencing the CoM. Walking speed largely influences the (relative) time spent in DS (Adamczyk and Kuo, 2009; Smith and Lemaire, 2018; Vlutters et al., 2016; Wu et al., 2019). When walking at a preferred speed, DS takes in total around 20 % of the gait cycle (Blanc et al., 1999; Kirtley et al., 1985). However, when the walking speed decreases to $0.63\,m\,s^{-1}$ or $0.10\,m\,s^{-1}$, the relative time spent in DS increases to 30 % and 56 % respectively (Vlutters et al., 2016; Wu et al., 2019). This lower speed becomes relevant in rehabilitation settings with stroke survivors (Titianova et al., 2003) or spinal cord injury subjects walking

* Corresponding author.
E-mail address: m.vanmierlo@utwente.nl (M. van Mierlo).

https://doi.org/10.1016/j.jbiomech.2021.110637
Accepted 31 May 2021
Available online 17 July 2021

Nomenclature

$\ddot{x}_{CoM}$	CoM acceleration in the sagittal plane
$\dot{H}$	Change in total body angular momentum in the sagittal plane
$\dot{x}_{CoM}$	CoM velocity in the sagittal plane
D_{CoP}	Centre of pressure range
g	Gravitational acceleration
l	Pendulum length
m	Subject mass
T_{DS}	Double support duration
T_{MR}	Relative-time at mid-range
$x_{CoP-CoM}$	Horizontal distance between CoP and CoM in the sagittal plane
x_{CoM}	CoM position in the sagittal plane
AP	Anteroposterior
BoS	Base of Support
CoM	Centre of Mass
CoP	Centre of Pressure
DS	Double Support
GRF	Ground Reaction Force
LIPM	Linear Inverted Pendulum Model
ML	Mediolateral
SS	Single Support
TO	Toe Off

with an exoskeleton (Louie et al., 2015). Therefore, the period when both feet touch the ground seems to provide a window of opportunities to control balance by CoP modulations.

A simple linearized inverted pendulum model (LIPM) can be used to gain insight into the theoretical possibilities for balance recovery during human walking. This model describes the linear relationship between the horizontal CoP–CoM distance and the CoM acceleration. When the CoP is located posterior of the CoM, the GRF can accelerate the CoM forward, whereas the CoM can be decelerated when the CoP is located anterior of the CoM (Jian et al., 1993; Winter, 1995). Though this model is often used to describe single support (SS), we investigated its application during DS, to better understand of the effects of CoP modulations on the CoM motion.

The first aim of this study is to investigate how healthy subjects modulate their CoP of the total GRF beneath both feet in the sagittal plane during DS to recover from backward and forward pelvis perturbations during slow and normal walking. It is expected that these modulations will be related to the corrections of the CoM velocity during DS in order to maintain balance. The second aim is to understand how CoP modulations affect the CoM velocity and position, by model simulations. Finally the model will be used to analyse the feasible solutions for a full recovery and whether the human subjects utilized these required strategies.

2. Methods

2.1. Experimental data

We used data from ten healthy volunteers (five men, age 25 ± 2 yr, weight 67 ± 12 kg, height 1.80 ± 0.11 m, means ± SD) walking on a treadmill while being perturbed, collected in Vlutters et al. (2016). All subjects gave written informed consent in accordance with the Declaration of Helsinki. The subjects walked on a dual-belt instrumented treadmill (custom Y-Mill, Motekforce Link, Culemborg, The Netherlands), while 3D GRFs and moments were being recorded. Kinematic data was recorded with a 12-camera motion capture system (Visualeyez II, Phoenix Technologies, Burnaby, Canada). Nine rigid bodies with three LEDs were placed on the feet, lower legs, upper legs, pelvis, sternum and head. Single LEDs were located on the lateral epicondyles of the knees and lateral malleoli. Prior to the experiment, a probe was used to take kinematic measures of the bony landmarks (calcaneus, first and fifth metatarsal heads, medial and lateral malleoli, fibula head, medial and lateral epicondyles of the femur, greater trochanter, anterior and posterior superior iliac spines, xiphoid process, jugular notch, seventh cervical vertebra, occiput, head vertex and nasal sellion). The subjects walked at a slow speed of $0.63 \cdot \sqrt{l}$ m s^{-1} and normal speed of $1.25 \cdot \sqrt{l}$ m s^{-1}, were l is the subjects leg length. AP pelvis perturbations where given with a motor (SMH60, Moog, Nieuw-Vennep, The Netherlands) placed behind the treadmill. Perturbations were given with a magnitude of 4, 8, 12 and 16 % of the subject's body weight at toe off (TO) right. Each perturbation lasted 150 ms and was repeated eight times in a random order. Due to attachments to the perturbation device the arms were crossed over the abdomen. A detailed description of the equipment, setup and protocol, approved by the local ethics committee, can be found in Vlutters et al. (2016).

2.2. Processing experimental data

Data were processed with Matlab (R2019b, MathWorks). The marker and force data were filtered with a fourth-order 6 Hz zero-phase low-pass Butterworth filter. The whole-body AP CoM position (x_{CoM}) was derived from the marker data according to Dumas et al. (2007). This was differentiated and the belt velocity was added to get the CoM velocity ($\dot{x}_{CoM}$). The total AP CoP position (x_{CoP}) was derived from the GRF and moment data of both feet together. Gait phases based on TO and heel strike events where detected with the minimal and maximal x_{CoP} (Roerdink et al., 2008). All data were normalized with the subjects' leg length according to Hof (1996) and multiplied with the average leg length over all subjects, to allow for physical interpretation. The first DS after a perturbation was analysed, when the left foot was trialing and right foot leading. A time normalization was done, allowing averaging of the data across all repetitions within each subject, followed by calculating the average and standard deviation across all subjects.

2.3. Experimental outcome variables

Three variables were retrieved from the experimental data to describe the duration, length and shape of the total DS x_{CoP} trajectory as result of the GRF beneath both feet (Fig. 1). The DS duration (T_{DS}) is the time DS lasts. The CoP range (D_{CoP}) is the distance between the initial and final DS x_{CoP}. This is determined by the step location and possibilities for CoP positioning below the feet. The relative-time at mid-range (T_{MR}) is the fraction of T_{DS} when half of D_{CoP} is reached, describing whether loading of the leading leg is done early or late during DS. For each perturbation direction and walking speed the correlation coefficient and its statistical significance were calculated between the CoP variables and the change in $\dot{x}_{CoM}$ over the DS phase ($\Delta\dot{x}_{CoM}$).

2.4. Model

A 2D LIPM was implemented in Simulink (Matlab R2019b, MathWorks), to model the effects of CoP modulations on x_{CoM} and $\dot{x}_{CoM}$. The relationship is described by:

$$\ddot{x}_{CoM} = \frac{g}{l} \cdot x_{CoP-CoM} - \frac{1}{m \cdot l} \cdot \dot{H} \quad (1)$$

in which $\ddot{x}_{CoM}$ is the AP CoM acceleration, g is the gravitational acceleration, l is the pendulum length, $x_{CoP-CoM}$ is the AP distance between the CoP and CoM, m is the subjects mass and $\dot{H}$ is the change in total body angular momentum with respect to the CoM (Fig. 2) (Hof, 2007; Jian et al., 1993). A generated x_{CoP} trajectory (Section 2.5)

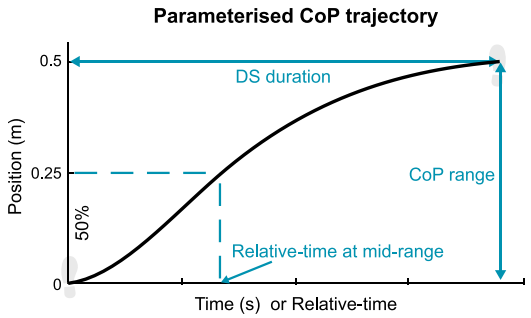

Fig. 1. Parameterized CoP trajectory with the three variables: DS duration (T_{DS}), CoP range (D_{CoP}) and relative-time at mid-range (T_{MR}), which is the fraction of the total T_{DS} when half of the D_{CoP} is reached. The graph presents the CoP position of the total GRF, in one direction over time, with the initial position beneath the trailing foot at 0 m and ending beneath the leading foot at the end of DS.

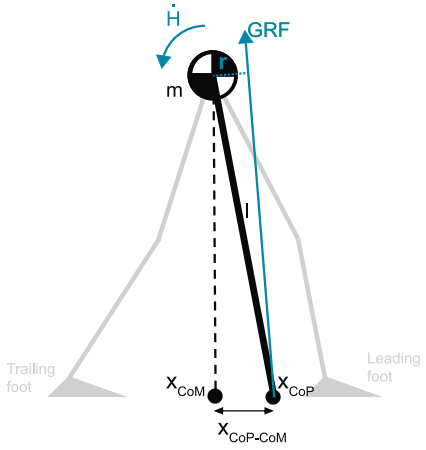

Fig. 2. LIPM with a point mass m and leg length l. CoP is the AP position of the total CoP between the trailing and leading foot, the $x_{CoP-CoM}$ is the distance between horizontal projection of the CoM and the CoP. $\dot{H}$ is the change in angular momentum, as result from the GRF not passing through the CoM. It was calculated by multiplying magnitude of the GRF vector and the moment arm r between the GRF vector and CoM.

was used as input for the model, figure S1. The outputs were the x_{CoM} and $\dot{x}_{CoM}$ time series. Constants provided to the model were the average subjects' CoM height (0.99 m) and mass (67 kg). Initial conditions included the $\dot{x}_{CoM}$ and $x_{CoP-CoM}$. Experimental unperturbed time series were used for $\dot{H}$. The constants, initial conditions and $\dot{H}$ all came from averages of the experimental data across all subjects. Details of our LIPM evaluation in the sagittal plane during DS can be found in the supplementary material. The simulated x_{CoM} and $\dot{x}_{CoM}$ for the slow walking speed resembled the experimental trajectories, with final DS errors respectively ranging from −5.6 mm to 2.9 mm and from $-0.03\,\mathrm{m\,s^{-1}}$ to $0.03\,\mathrm{m\,s^{-1}}$.

2.5. Model sensitivity for individual parameters

To identify the effects of modulations of both individual CoP variables and variable combinations on the x_{CoM} and $\dot{x}_{CoM}$, a cubic spline function was used to generate parameterized CoP trajectories. Table 1 presents the limits of the parameter values for the T_{DS}, D_{CoP} and T_{MR}, based on realistic limits for a walking speed of $0.63\cdot\sqrt{l}\ \mathrm{m\,s^{-1}}$. The T_{DS} was limited by the maximum time the CoM can move forward without passing the leading foot. The D_{CoP} was based on the average distance between the initial and final DS x_{CoP} from the experimental data, basically the step length and dimensions of the feet. The spline function limited the T_{MR} possibilities, since the shape of the created curve deviated from the experimental CoP trajectories for values outside the

Table 1
Parameter limits for the generated CoP trajectories in the sagittal plane, retrieved from the experimental data.

	DS duration (s)	CoP range (m)	Relative-time at mid-range
Minimum	0	0.30	0.25
Maximum	0.38	0.55	0.75

Table 2
Initial values for the model based on average experimental data at the beginning of DS of the unperturbed condition and after 16 % backward and forward perturbations (Vlutters et al., 2016).

	Unperturbed	16 % forward	16 % backward
$\dot{x}_{CoM}$ ($\mathrm{m\,s^{-1}}$)	0.61	0.85	0.55
$x_{CoM-CoP}$ (m)	0.09	0.14	0.15

selected limits. For each variable 15 values were taken, equally spaced between these limits, resulting in 15^3 parameterized CoP trajectories. The x_{CoM} and $\dot{x}_{CoM}$ trajectories were simulated for all these generated CoP trajectories, with initial values based on average values originating from the experimental data of three conditions (unperturbed walking, 16 % forward and 16 % backward perturbations), see Table 2.

2.6. Comparison feasible and utilized CoP modulations

We investigated which sets of parameter combinations were able to bring the modelled CoM state (x_{CoM} and $\dot{x}_{CoM}$) back to desired values at the end of DS. As desired values we defined the final DS CoM state originating form experimental data ±5 %. This was either from the corresponding perturbation condition, or from the unperturbed walking condition to see whether there are options to return to baseline within the first DS after a perturbations. The combinations of CoP parameters originating from the experimental data were compared to the theoretical feasible solutions.

3. Results

3.1. Experimental centre of pressure modulations

During unperturbed walking, humans use a propulsion strategy to increase the $\dot{x}_{CoM}$ over DS, Fig. 3. Perturbations given at the moment of TO affect the initial $\dot{x}_{CoM}$ of the following DS. Backward perturbations decreased the initial $\dot{x}_{CoM}$. For the strongest perturbations this decrease was $0.12\,\mathrm{m\,s^{-1}}$ and $0.06\,\mathrm{m\,s^{-1}}$ for the normal and slow walking speed respectively. The subjects used a propulsion strategy to increase the $\Delta\dot{x}_{CoM}$ to bring the $\dot{x}_{CoM}$ back towards the unperturbed value. Compared to backward perturbations, the effects of forward perturbations on the initial DS $\dot{x}_{CoM}$ are larger, with an increase of $0.28\,\mathrm{m\,s^{-1}}$ for the normal and $0.24\,\mathrm{m\,s^{-1}}$ for the slow walking speed. After the strongest perturbations the subjects even showed a braking strategy decreasing $\Delta\dot{x}_{CoM}$, especially during slow walking.

Subjects modulated the T_{DS}, D_{CoP} and T_{MR} of the x_{CoP} trajectory after perturbations given at TO, depending on the walking speed and perturbation direction and magnitude, Fig. 4. After forward perturbations these modulations were strongly correlated to the $\Delta\dot{x}_{CoM}$, Fig. 5. Forward perturbations resulted in a shorter T_{DS}, larger D_{CoP} and earlier T_{MR}, related to a decrease of the $\Delta\dot{x}_{CoM}$, and even a braking strategy after the strongest perturbations, opposing the perturbation. Backward perturbations did not result in consistent correlations between the CoP variables and the $\Delta\dot{x}_{CoM}$. This could be explained by the smaller deviation of $\dot{x}_{CoM}$ at the beginning of DS, requiring less propulsion during DS.

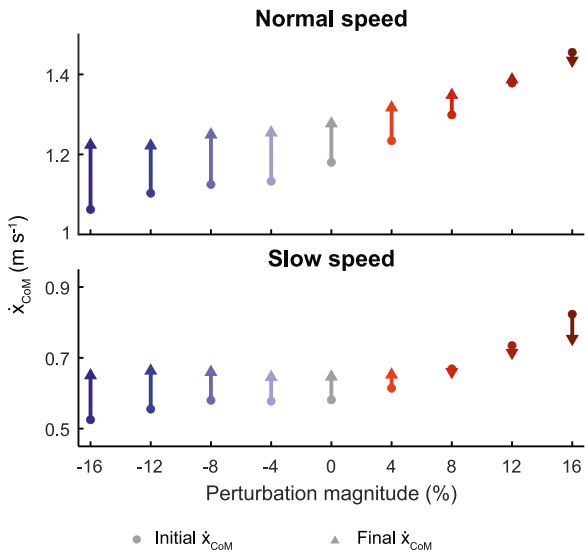

Fig. 3. The initial (dots) and final (triangles) DS CoM velocities ($\dot{x}_{CoM}$) after different perturbation magnitudes given at previous TO, of the experimental data. The size of the arrow indicates the $\Delta\dot{x}_{CoM}$ over the DS phase. The top row presents the data during a normal walking speed and the bottom row for a slow walking speed.

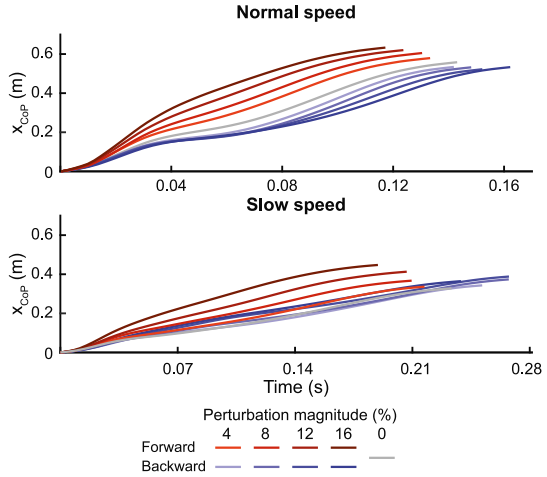

Fig. 4. Experimental trajectories of the CoP of the total GRF beneath both feet during DS of walking with a normal and slow speed, in AP direction after backward and forward perturbations. The colour gradient indicates the magnitude of the perturbation. (For interpretation of the references to colour in this figure legend, the reader is referred to the web version of this article.)

3.2. Model sensitivity for individual parameters

The simulations showed that modulating the individual CoP parameters contributed to either a braking or propulsion strategy (Fig. 6). Compared to the other parameters, modulations of the T_{DS} had the largest effect on the Δx_{CoM}, which increased for longer T_{DS}, supporting propulsion. The effect of T_{DS} on the $\Delta\dot{x}_{CoM}$ showed a turning point around 0.12 s, shorter and longer T_{DS} resulted in larger $\Delta\dot{x}_{CoM}$. Modulating the D_{CoP} and T_{MR} mainly affected the $\Delta\dot{x}_{CoM}$, while minimally affecting the Δx_{CoM}. Larger D_{CoP} resulted in more negative $\Delta\dot{x}_{CoM}$ and a small decrease of the Δx_{CoM}. A later T_{MR} resulted in an increase of the Δx_{CoM} and $\Delta\dot{x}_{CoM}$, because braking was introduced later.

3.3. Comparison feasible and utilized CoP modulations

Simulating the x_{CoM} and $\dot{x}_{CoM}$ based on parameterized CoP trajectories showed various combinations of the three parameters that are able to bring the CoM back to the corresponding experimental final DS condition in the sagittal plane (left column Fig. 7). As expected, the parameter combinations used by the human subjects also fall within these possibilities for both the backward and forward perturbations. Alternative combinations involving a larger D_{CoP} required a later T_{MR} to realize comparable effects. Backward perturbations required a later T_{MR} and longer T_{DS} compared to forward perturbations. For almost all D_{CoP}, combinations were found resulting in the desired CoM state. Bringing the CoM state back to the unperturbed final DS condition, full recovery, required more extreme parameter values (right column Fig. 7). These contained shorter T_{DS} for both perturbation directions. Forward perturbations required an earlier T_{MR} and the backward perturbations a later T_{MR}. The experimental data showed that the subjects where not utilizing these extreme modulations.

4. Discussion

The study goal was to gain insights into the theoretically possible and actually used CoP modulations for balance recovery in the sagittal plane during DS. The relation between CoP trajectory modulations and the x_{CoM} and $\dot{x}_{CoM}$ during DS were studied in human subjects and simulated data. In order to counteract the perturbation, subjects modulated the shape, length and duration of the x_{CoP} trajectory to induce braking or propulsion, depending on the magnitude and direction of the perturbation and walking speed. The simulated data showed how braking and propulsion could be achieved by modulating the CoP parameters and which parameter combinations can bring the Δx_{CoM} and $\Delta\dot{x}_{CoM}$ back to a desired final DS value.

4.1. Experimental centre of pressure modulations

Following forward perturbations, returning to the unperturbed condition requires braking to reduce the $\dot{x}_{CoM}$, while after backward perturbations propulsion is needed to increase the $\dot{x}_{CoM}$, figure 3 from Vlutters et al. (2016). During DS this can be done by modulating the x_{CoP} trajectory, either through an ankle torque or weight shift (Hof, 2007). We made no distinction between these contributions, but focused on the total CoP modulations in the sagittal plane in terms of three selected variables. After forward perturbations, the modulations of these variables were correlated to the $\Delta\dot{x}_{CoM}$, to oppose the effect of the perturbations on the $\dot{x}_{CoM}$. However, this correlation was absent after the backward perturbations, while the subjects were still able to correct the $\dot{x}_{CoM}$. An explanation can be that for backward perturbations a larger correction was already done before entering DS, which is also suggested in figure 5 from Vlutters et al. (2018). The plantarflexion ankle moment decreased and even a dorsiflexion moment was created after stronger backward perturbations, while the plantarflexion moment was already saturated after small forward perturbations (Vlutters et al., 2018).

The T_{MR} describes whether loading of the leading leg is done early or late during DS. Early loading of the leading leg means that the x_{CoP} is shifted anteriorly early during DS. According to the LIPM, the $\dot{x}_{CoM}$ decreases when the x_{CoP} is located anterior of the x_{CoM} (Jian et al., 1993). This braking strategy was also shown in a study by Matjačić et al. in the frontal plane after mediolateral (ML) perturbations (Matjačić et al., 2020). In our study the subjects loaded the leading leg earlier to reduce the $\dot{x}_{CoM}$ after forward perturbations. This was even more effective during slow walking, probably due to the longer T_{DS}, giving more time to adjust the $\dot{x}_{CoM}$. Remarkably, after backward perturbations during slow walking the $\Delta\dot{x}_{CoM}$ increased for earlier T_{MR}. This seems counterintuitive, but to distinguish between acceleration and deceleration of the CoM, it is relevant whether the CoP is located behind or in front of the CoM, which is not captured with the T_{MR}. After backward perturbations, the CoP and CoM crossing occurred later than the T_{MR}, meaning that more time was used to accelerate the CoM forward.

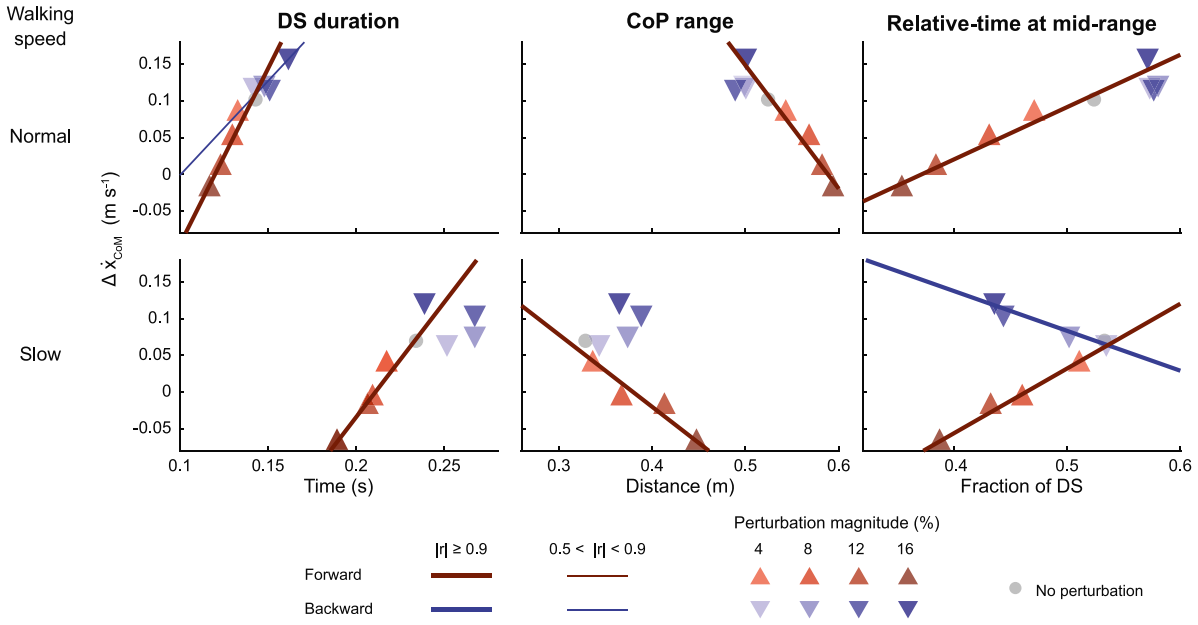

Fig. 5. Correlations in the experimental data between the three CoP variables (T_{DS}, D_{CoP} and T_{MR}) and the change in CoM velocity over the DS in AP direction ($\Delta\dot{x}_{CoM}$). The relationships are presented for either a normal (top row) or slow (bottom row) walking speed. Average data across all subjects is presented with triangles, pointing in the direction of the perturbation and with a colour gradient indicating the magnitude of the perturbation. Lines are only drawn for the correlations with a p-value < 0.05 and a correlation coefficient of either $0.7 < |r| < 0.9$ (thin line) or $|r| \geq 0.9$ (thick line). The blue lines correspond to the backward and the red to the forward perturbations. (For interpretation of the references to colour in this figure legend, the reader is referred to the web version of this article.)

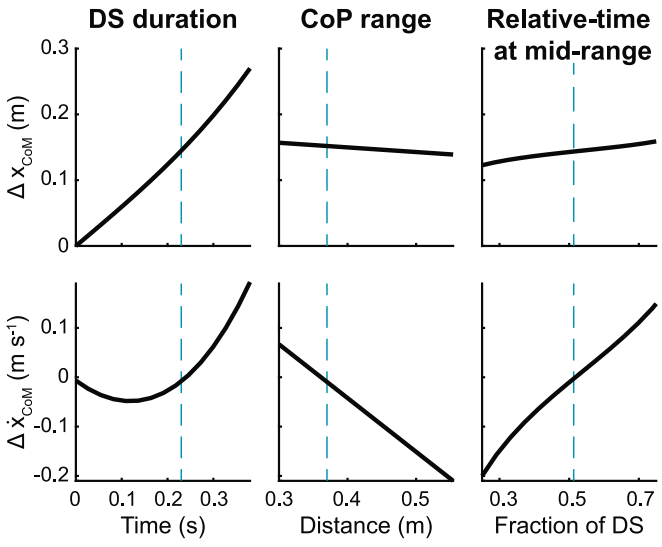

Fig. 6. Model results: the effects of modulations of individual CoP parameters (T_{DS}, D_{CoP} and T_{MR}) on the Δx_{CoM} and $\Delta\dot{x}_{CoM}$ in the sagittal plane. For modulations of one of the parameters, the remaining two were set to average experimental value indicated with the vertical dotted line.

After forward perturbations modulations of the T_{DS} and D_{CoP} were seen, which were correlated to the $\Delta\dot{x}_{CoM}$. Making the T_{DS} shorter and increasing the D_{CoP} resulted in a decrease of the propulsion, and even braking after the strongest perturbations. This could be caused by the shorter time to increase the $\dot{x}_{CoM}$ over DS. These correlations were absent after backward perturbations. Probably due to the larger variability of the T_{DS} and D_{CoP} after backward perturbations. It seems multiple strategies could be used after the backward perturbations to maintain balance. This was also evidenced by others presenting kinematic constraints requiring alternative adjustments, and variation in muscle activation responses (Vlutters et al., 2018; Mihelj et al., 2000).

4.2. Model sensitivity for individual parameters

The model suggests that correcting for a balance perturbation in terms of braking the $\dot{x}_{CoM}$ can be most efficiently done by bringing the x_{CoP} early to the front and bringing it further to the front. These modulations influence $x_{CoP-CoM}$, which directly affects the $\ddot{x}_{CoM}$, resulting in an increase or decrease of the $\dot{x}_{CoM}$ (Jian et al., 1993). The x_{CoM} was mostly affected by the T_{DS}. Moving forward for a shorter or longer time, mainly determines the CoM displacement. This makes the final DS CoM state sensitive to changes in all three CoP parameters and explains the used CoP modulations by the human subject after the forward perturbations.

4.3. Comparison feasible and utilized CoP modulations

CoP modulations observed in humans after backward and forward perturbations fall within the feasibilities predicted by the LIPM. According to the simulated data a desired $\dot{x}_{CoM}$ and x_{CoM} at the end of DS can also be obtained with various other CoP modulations. Remarkably, for both perturbation directions only a small range of T_{DS} values were possible compared to the other parameters, which is probably caused by dominant influence of the T_{DS} on the desired final x_{CoM}.

Compared to forward perturbations, after backward perturbations a larger variety of combinations can be used to reach the desired final DS CoM state. For these perturbations a larger correction was already done during the previous swing phase, leaving a smaller deviating $\dot{x}_{CoM}$ to correct for during DS. Many combinations could therefore be used to make these small corrections. This large amount of possibilities could explain the inconsistency in the use of CoP modulations seen in the experimental data after backward perturbations, causing the absence of correlations between the CoP variables and the $\Delta\dot{x}_{CoM}$.

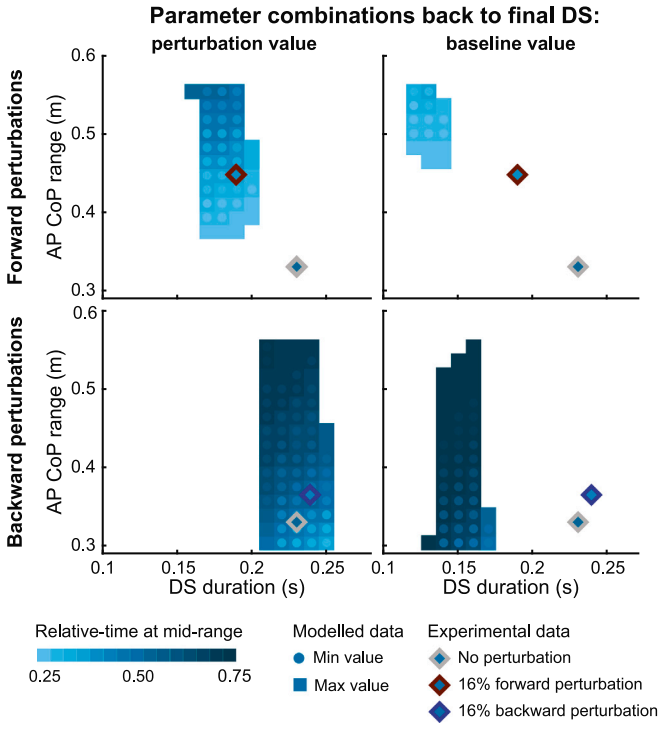

Fig. 7. Model results of combinations of the three parameters T_{DS}, D_{CoP} and T_{MR} resulting in the desired x_{CoM} and $\dot{x}_{CoM}$ at the end of DS. The parameter values for T_{DS} and D_{CoP} are shown at the axes, the third parameter, T_{MR}, is presented with the colour of the markers. The top row presents the forward perturbations and the bottom row the backward perturbations. For the left column the desired value is the experimental final DS x_{CoM} and $\dot{x}_{CoM}$ of the corresponding perturbation condition and for the right column it is the unperturbed condition. The squares indicate the maximum value of the possible T_{MR} and the circles the minimum value. A large colour difference between each square and circle indicates a large range of possible T_{MR} values. A small or no difference indicates a small range of possible T_{MR} values. Used parameter combinations in the experimental data are shown with the diamonds, these have the same value in the left and right column. (For interpretation of the references to colour in this figure legend, the reader is referred to the web version of this article.)

Though subjects did not return the x_{CoM} and $\dot{x}_{CoM}$ to the unperturbed state at the end of the first DS after a perturbation, the model suggest that it is feasible. More extreme modulations of the CoP were required for the return to this condition in the sagittal plane. Remarkably is the short T_{DS}, since less adjustments can be made to the $\Delta\dot{x}_{CoM}$ for shorter T_{DS}. The extreme early and late T_{MR} after the forward and backward perturbations respectively, can compensate for this. However, humans did not adopt this strategy for several reasons. First, when there is no immediate threat of falling anymore, the following gait phases can also be used to complete the recovery. Therefore, humans might choose the most energetically efficient gait pattern (Kuo et al., 2005), over the quickest. Second, a quicker might even not be possible because of muscle constraints limiting a faster generation of joint torques. A third reason could be the coupling with the frontal plane. For both planes the DS duration is of course the same. Also, the required changes to recover in AP direction might have negative effects in ML direction, which have not been addressed with our 2D simulations in the sagittal plane. Previous studies have indeed shown that adjustments to counteract ML perturbations were accompanied by adjustments in the AP direction (Matjačić et al., 2020; Vlutters et al., 2016) and vice versa (Vlutters et al., 2018).

4.4. Limitations

The use of the LIPM during the DS might be questioned. The representation with a single pendulum consisting of a point mass and massless leg might be too simple during this phase (Adamczyk and Kuo, 2009; Antoniak et al., 2019; Donelan et al., 2002; McGrath et al., 2015; Reimann et al., 2017). However, evaluation of the LIPM during DS, reported in the supplementary material, showed results comparable to the experimental data. The remaining errors might be caused by the simple LIPM not being able to cover the nonlinearities and components influencing the relationship between the CoP and CoM (Kim and Collins, 2017).

To simulate the effect of CoP modulations on the CoM state we used only three parameters and a spline function to generate realistic trajectories. Making use of more parameters will give better imitations of real CoP trajectories. However, this will complicate the physical interpretation and analysis of the individual parameters as well.

Conclusion

Humans modulate the length, shape and duration of the DS CoP trajectory to control the CoM position and velocity for balance recovery in the sagittal plane. Simulations showed how these modulations resulted in more or less propulsion and braking to counteract the effects of the perturbations. This even suggests possibilities for a complete balance recovery within DS, which were not utilized by the human subjects. Modulating the DS duration effectively controls the change in CoM position over DS, while early or late loading of the leading leg and the travelled CoP distance mainly control the CoM velocity.

CRediT authorship contribution statement

M. van Mierlo: Conceptualization, Methodology, Software, Formal analysis, Writing – original draft, Visualization. **M. Vlutters:** Conceptualization, Methodology, Software, Investigation, Writing – review & editing. **E.H.F. van Asseldonk:** Conceptualization, Methodology, Writing – original draft, Writing – review & editing, Supervision. **H. van der Kooij:** Conceptualization, Methodology, Writing – review & editing, Supervision, Project administration, Funding acquisition.

Declaration of competing interest

The authors declare that they have no known competing financial interests or personal relationships that could have appeared to influence the work reported in this paper.

Acknowledgements

This work is part of the research program Wearable Robotics with project number P16-05, which is (partly) funded by the Dutch Research Council (NWO).

Appendix A. Supplementary data

Supplementary material related to this article can be found online at https://doi.org/10.1016/j.jbiomech.2021.110637.

References

Adamczyk, P.G., Kuo, A.D., 2009. Redirection of center-of-mass velocity during the step-to-step transition of human walking. J. Exp. Biol. 212 (16), 2668–2678. http://dx.doi.org/10.1242/jeb.027581.

Antoniak, G., Biswas, T., Cortes, N., Sikdar, S., Chun, C., Bhandawat, V., 2019. Spring-loaded inverted pendulum goes through two contraction-extension cycles during the single-support phase of walking. Biol. Open 8 (6), 1–11. http://dx.doi.org/10.1242/bio.043695.

Arvin, M., Hoozemans, M.J., Pijnappels, M., Duysens, J., Verschueren, S.M., van Dieën, J.H., 2018. Where to step? Contributions of stance leg muscle spindle afference to planning of mediolateral foot placement for balance control in young and old adults. Front. Physiol. 9 (1134), 1–10. http://dx.doi.org/10.3389/fphys.2018.01134.

Blanc, Y., Balmer, C., Landis, T., 1999. Temporal parameters and patterns of the foot roll over during walking. Gait Posture 10, 97–108.

Bruijn, S.M., Dieën, J.H.V., 2018. Control of human gait stability through foot placement. J. R. Soc. Interface 15, http://dx.doi.org/10.1098/rsif.2017.0816.

Donelan, J.M., Kram, R., Kuo, A.D., 2002. Mechanical work for step-to-step transitions is a major determinant of the metabolic cost of human walking. J. Exp. Biol. 205 (23), 3717–3727.

Dumas, R., Chèze, L., Verriest, J.-P., 2007. Adjustments to McConville et al. and Young et al. body segment inertial parameters. J. Biomech. 40, 543–553. http://dx.doi.org/10.1016/j.jbiomech.2006.02.013.

Gruben, K.G., Boehm, W.L., 2014. Ankle torque control that shifts the center of pressure from heel to toe contributes non-zero sagittal plane angular momentum during human walking. J. Biomech. 47 (6), 1389–1394. http://dx.doi.org/10.1016/j.jbiomech.2014.01.034.

Hof, A., 1996. Scaling gait data to body size. Gait 4, 222–223.

Hof, A.L., 2007. The equations of motion for a standing human reveal three mechanisms for balance. J. Biomech. 40 (2), 451–457. http://dx.doi.org/10.1016/j.jbiomech.2005.12.016.

Hof, A.L., Duysens, J., 2013. Responses of human hip abductor muscles to lateral balance perturbations during walking. Exp. Brain Res. 230 (3), 301–310. http://dx.doi.org/10.1007/s00221-013-3655-5.

Hof, A.L., Gazendam, M.G., Sinke, W.E., 2005. The condition for dynamic stability. J. Biomech. 38 (1), 1–8. http://dx.doi.org/10.1016/j.jbiomech.2004.03.025.

Hof, A.L., Vermerris, S.M., Gjaltema, W.A., 2010. Balance responses to lateral perturbations in human treadmill walking. J. Exp. Biol. 213, 2655–2664. http://dx.doi.org/10.1242/jeb.042572.

Jian, Y., Winter, D., Ishac, M., Gilchrist, L., 1993. Trajectory of the body COG and COP during initiation and termination of gait. Gait Posture 1 (1), 9–22. http://dx.doi.org/10.1016/0966-6362(93)90038-3.

Kim, M., Collins, S.H., 2017. Once-per-step control of ankle push-off work improves balance in a three-dimensional simulation of bipedal walking. IEEE Trans. Robot. 33 (2), 406–418. http://dx.doi.org/10.1109/TRO.2016.2636297.

Kirtley, C., Whittle, M.W., Jefferson, R.J., 1985. Influence of walking speed on gait parameters. J. Biomed. Eng. 7 (4), 282–288. http://dx.doi.org/10.1016/0141-5425(85)90055-X.

Kuo, A.D., Donelan, J.M., Ruina, A., 2005. Energetic consequences of walking like an inverted pendulum: Step-to-step transitions. Exercise Sport Sci. Rev. 33 (2), 88–97. http://dx.doi.org/10.1097/00003677-200504000-00006.

Louie, D.R., Eng, J.J., Lam, T., Cord, S., Scire, E., 2015. Gait speed using powered robotic exoskeletons after spinal cord injury: a systematic review and correlational study. J. Neuroeng. Rehabil. 1–10.

Matjačić, Z., Zadravec, M., Olenšek, A., 2017. An effective balancing response to lateral perturbations at pelvis level during slow walking requires control in all three planes of motion. J. Biomech. 60, 79–90. http://dx.doi.org/10.1016/j.jbiomech.2017.06.020.

Matjačić, Z., Zadravec, M., Olenšek, A., 2020. Biomechanics of in-stance balancing responses following outward-directed perturbation to the pelvis during very slow treadmill walking show complex and well-orchestrated reaction of central nervous system. Front. Bioeng. Biotechnol. 8 (July), 1–14. http://dx.doi.org/10.3389/fbioe.2020.00884.

McGrath, M., Howard, D., Baker, R., 2015. The strengths and weaknesses of inverted pendulum models of human walking. Gait Posture 41 (2), 389–394. http://dx.doi.org/10.1016/j.gaitpost.2014.10.023.

Mihelj, M., Matjačić, Z., Bajd, T., 2000. Postural activity of constrained subject in response to disturbance in sagittal plane. Gait Posture 12 (2), 94–104. http://dx.doi.org/10.1016/S0966-6362(00)00065-5.

Millard, M., Wight, D., McPhee, J., Kubica, E., Wang, D., 2009. Human foot placement and balance in the sagittal plane. J. Biomech. Eng. 131 (12), 1–7. http://dx.doi.org/10.1115/1.4000193.

Pollock, A.S., Durward, B.R., Rowe, P.J., 2000. What is balance? Clin. Rehabil. 14, 402–406.

Reimann, H., Fettrow, T.D., Thompson, E.D., Agada, P., McFadyen, B.J., Jeka, J.J., 2017. Complementary mechanisms for upright balance during walking. PLoS One 12 (2), 1–16. http://dx.doi.org/10.1371/journal.pone.0172215.

Roerdink, M., Coolen, B.H.., Clairbois, B.H.E., Lamoth, C.J., Beek, P.J., 2008. Online gait event detection using a large force platform embedded in a treadmill. J. Biomech. 41 (12), 2628–2632. http://dx.doi.org/10.1016/j.jbiomech.2008.06.023.

Smith, A.J., Lemaire, E.D., 2018. Temporal-spatial gait parameter models of very slow walking. Gait Posture 61 (January), 125–129. http://dx.doi.org/10.1016/j.gaitpost.2018.01.003.

Titianova, E.B., Pitkänen, K., Pääkkönen, A., Sivenius, J., Tarkka, I.M., 2003. Gait characteristics and functional ambulation profile in patients with chronic unilateral stroke. Amer. J. Phys. Med. Rehabil. 82 (10), 778–786. http://dx.doi.org/10.1097/01.PHM.0000087490.74582.E0.

Tokur, D., Grimmer, M., Seyfarth, A., 2020. Review of balance recovery in response to external perturbations during daily activities. Hum. Mov. Sci. 69 (October 2019), 102546. http://dx.doi.org/10.1016/j.humov.2019.102546.

Vlutters, M., van Asseldonk, E.H.F., van der Kooij, H., 2016. Center of mass velocity-based predictions in balance recovery following pelvis perturbations during human walking. J. Exp. Biol. 219 (10), 1514–1523. http://dx.doi.org/10.1242/jeb.129338.

Vlutters, M., van Asseldonk, E.H.F., van der Kooij, H., 2018. Lower extremity joint-level responses to pelvis perturbation during human walking. Sci. Rep. 8 (1), 14621. http://dx.doi.org/10.1038/s41598-018-32839-8.

Winter, D.A., 1995. Human blance and posture control during standing and walking. Gait Posture 3 (4), 193–214. http://dx.doi.org/10.1016/0966-6362(96)82849-9.

Wu, A.R., Simpson, C.S., Asseldonk, E.H.F.V., Kooij, H.V.D., Ijspeert, A.J., 2019. Mechanics of very slow human walking. Sci. Rep. 1–10. http://dx.doi.org/10.1038/s41598-019-54271-2.